Luttinger liquid and persistent current in a continuous mesoscopic ring with a weak link

M. Moško,[1] R. Németh,[1,2] R. Krčmár,[1] and M. Indlekofer[3]
[1]*Institute of Electrical Engineering, Slovak Academy of Sciences, 841 04 Bratislava, Slovakia*
[2]*Institute for Bio and Nanosystems, CNI, Research Center Jülich, 52425 Jülich, Germany*
[3]*Wiesbaden, ING/ITE, University of Applied Sciences, 65428 Rüsselsheim, Germany*
(Received 18 February 2009; revised manuscript received 27 April 2009; published 23 June 2009)

The persistent current (I) of the spinless-electron Luttinger liquid is calculated by numerical microscopic methods in the continuous one-dimensional ring containing a weak link with transmission amplitude $\tilde{t}_{k_F} \ll 1$. The electrons interact via a screened interaction of range d. If $d \lesssim 1/2k_F$, the interaction modifies the transmission as $t_{k_F} \simeq \tilde{t}_{k_F} N^{-\alpha}$ and the current as $LI/ev_F \simeq |\tilde{t}_{k_F}| N^{-\alpha}$, where N is the electron number, L the ring length, N/L a fixed density, and α depends on the interaction in accord with the renormalization-group (RG) theory. Unlike our results, the RG theory predicts for a finite d the power laws $t_{k_F} \simeq \tilde{t}_{k_F}(L/d)^{-\alpha}$ and $LI/ev_F \simeq |\tilde{t}_{k_F}|(L/d)^{-\alpha}$, both depending on two interaction parameters, d and α. To explain why our results depend solely on α, we show analytically that the interaction-matrix elements depend only on α (not on d) when $d \lesssim 1/2k_F$. As d exceeds $1/2k_F$, our result for LI/ev_F starts to depend on d as well and likely approaches the result $LI/ev_F \simeq |\tilde{t}_{k_F}|(L/d)^{-\alpha}$ in the limit $L \gg d \gg 1/2k_F$, not feasible by our numerical methods.

DOI: 10.1103/PhysRevB.79.245323 PACS number(s): 73.23.−b, 71.10.Pm, 73.61.Ey

The electron-electron (e-e) interaction causes that the one-dimensional (1D) electron gas in a clean 1D wire away from the charge-density-wave instability is a Luttinger liquid.[1] The Luttinger-liquid state affects the electron conductance already when the wire contains a single scatterer. For noninteracting electrons the conductance is $(2e^2/h)|\tilde{t}_{k_F}|^2$, where $\tilde{t}_{k_F}$ is the transmission amplitude through the scatterer and k_F is the Fermi wave vector.[2] For the Luttinger liquid, the conductance of the infinite wire with a single impurity or weak link varies with temperature as $\propto T^{2\alpha}$, where α depends only on the e-e interaction.[3,4] For $\alpha > 0$ (repulsive interaction) such wire is impenetrable at $T \to 0$ K regardless of the strength of the scatterer. If $T=0$ K and the wire length (L) is finite, the conductance shows the power law $\propto L^{-2\alpha}$. These power laws are a sign of the Luttinger liquid. A similar power law results for interacting electrons in a mesoscopic ring. Magnetic flux piercing the opening of the isolated ring gives rise to the persistent electron current.[2] For the noninteracting spinless electrons in the 1D ring containing the weak link with transmission probability $|\tilde{t}_{k_F}|^2 \ll 1$, the persistent current at $T=0$ K depends on the magnetic flux ϕ and ring length L as[5]

$$I \simeq (ev_F/2L)|\tilde{t}_{k_F}|\sin(2\pi\phi/\phi_0), \tag{1}$$

where $\phi_0 = h/e$ and v_F is the Fermi velocity. However, for the Luttinger liquid one finds[5]

$$I \propto L^{-\alpha-1}\sin(2\pi\phi/\phi_0). \tag{2}$$

Renormalization-group (RG) theory[6] shows how the bare transmission amplitude $\tilde{t}_{k_F}$ of the scatterer in the 1D wire of length L is renormalized by weak e-e interaction. For large L the renormalized amplitude reads

$$t_{k_F} \simeq (\tilde{t}_{k_F}/|\tilde{r}_{k_F}|)(L/d)^{-\alpha}, \quad \alpha > 0, \tag{3}$$

where $|\tilde{r}_{k_F}|^2 = 1 - |\tilde{t}_{k_F}|^2$ and d is the range of the pair e-e interaction $V(x-x')$. The RG theory also shows that for the spinless weakly interacting system α coincides with

$$\alpha_{\rm RG} \equiv [V(0) - V(2k_F)]/2\pi\hbar v_F, \tag{4}$$

where $V(q)$ is the Fourier transform of $V(x-x')$. More precisely,[6] $\alpha = \alpha_{\rm RG}$ for $\alpha_{\rm RG} \ll 1$. For strong interaction (say $\alpha_{\rm RG} \simeq 0.5$) the theory[1,7] predicts the result

$$\alpha = (1 + 2\alpha_{\rm RG})^{1/2} - 1. \tag{5}$$

The power law (2) follows heuristically[5] from Eq. (1), if we replace $\tilde{t}_{k_F}$ by the renormalized t_{k_F}. We get the formula

$$I \simeq \frac{ev_F}{2L}\frac{|\tilde{t}_{k_F}|}{|\tilde{r}_{k_F}|}(L/d)^{-\alpha}\sin(2\pi\phi/\phi_0), \quad \alpha > 0, \tag{6}$$

which provides an estimate of the proportionality factor in Eq. (2) and involves α given by formulas (4) and (5).

In this work we analyze the circular 1D ring of length L threaded by magnetic flux ϕ with N interacting spinless electrons described by the Hamiltonian

$$\hat{H} = \sum_{j=1}^{N}\left[\frac{\hbar^2}{2m}\left(\frac{1}{i}\frac{\partial}{\partial x_j} + \frac{2\pi}{L}\frac{\phi}{\phi_0}\right)^2 + \gamma\delta(x_j)\right] + \frac{1}{2}\sum_{\substack{i,j=1\\ i\neq j}}^{N} V(x_j - x_i), \tag{7}$$

where x_j is the coordinate of the jth electron,

$$V(x_j - x_i) = V_0 \exp(-|x_j - x_i|/d) \tag{8}$$

is the screened e-e interaction, and $\gamma\delta(x)$ is the potential due to the weak link. We solve the Schödinger equation

$$\hat{H}\Psi(x_1, x_2, \ldots, x_N) = E\Psi(x_1, x_2, \ldots, x_N) \tag{9}$$

with the boundary condition $\Psi(x_1, \ldots, x_i + L, \ldots, x_N) = \Psi(x_1, \ldots, x_i, \ldots, x_N)$ by numerical microscopic methods. In turn, we calculate the persistent current at $T=0$ K,

$$I = \langle \Psi_0 | \hat{I} | \Psi_0 \rangle, \tag{10}$$

where $\hat{I} = -\frac{e}{mL}\sum_{j=1}^{N}(\frac{\hbar}{i}\frac{\partial}{\partial x_j} + \frac{e\phi}{L})$ is the current operator and $\Psi_0(x_1, x_2, \ldots, x_N)$ is the ground-state wave function.

Our major goal is to verify formulas (4) and (5). The formulas predict the same α for many various functions $V(x-x')$ with the same value of α_{RG}. In our continuous model, this prediction can be verified by smoothly varying the parameters V_0 and d while keeping the same α_{RG}. This cannot be achieved in the lattice-model-based microscopic studies[8–11] with a fixed (on-site or nearest-neighbor-site) interaction. Another distinction in comparison with previous many-body models[3,5,6,8–11] is that in our model the energy band is parabolic ($\propto k^2$).

Our major result is that for $d \lesssim 1/2k_F$ the persistent current exhibits the asymptotic (large N) dependence

$$I = C\frac{ev_F}{2L}\frac{|\tilde{t}_{k_F}|}{|\tilde{r}_{k_F}|}N^{-\alpha}\sin(2\pi\phi/\phi_0), \quad \alpha > 0, \tag{11}$$

where N/L is a fixed density, $C = 1+1.66\alpha$, and α agrees with formulas (4) and (5). Formula (11) implies the power laws $LI/ev_F \simeq |\tilde{t}_{k_F}|N^{-\alpha}$ and $t_{k_F} \simeq \tilde{t}_{k_F}N^{-\alpha}$ which depend on a single interaction parameter (α) while power laws (6) and (3) depend on α and d. As d exceeds $1/2k_F$, our result for LI/ev_F starts to depend on d as well and likely approaches result (6) in the limit $L \gg d \gg 1/2k_F$, not feasible by our methods. It is also interesting that the $N^{-\alpha}$ decay is reachable for $N \sim 10$.

We briefly outline our calculation, described in detail elsewhere.[12] We solve numerically the single-electron problem $[\frac{\hbar^2}{2m}(\frac{1}{i}\frac{\partial}{\partial x} + \frac{2\pi}{L}\frac{\phi}{\phi_0})^2 + \gamma\delta(x)]\psi_n(x) = \varepsilon_n\psi_n(x)$ with condition $\psi_n(x+L) = \psi_n(x)$. We construct the noninteracting N-particle states as the Slater determinants

$$\chi_n = \frac{1}{\sqrt{N!}}\begin{vmatrix} \psi_{n_1}(x_1) & \ldots & \psi_{n_N}(x_1) \\ \vdots & \ddots & \vdots \\ \psi_{n_1}(x_N) & \ldots & \psi_{n_N}(x_N) \end{vmatrix} \tag{12}$$

with eigenenergies $\mathcal{E}_n = \varepsilon_{n_1} + \cdots + \varepsilon_{n_N}$, where the quantum numbers $n_1, \ldots, n_N$ specify the single-particle states of the first, $\ldots$, Nth electron, respectively, and n labels the resulting N-particle state. Following the method of the configuration interaction (CI),[13,14] we expand Ψ as

$$\Psi = c_0\chi_0 + c_1\chi_1 + c_2\chi_2 + \cdots + c_M\chi_M + \ldots, \tag{13}$$

where $n = 0, 1, 2, \ldots$ corresponds to $\mathcal{E}_0 < \mathcal{E}_1 < \mathcal{E}_2 \ldots$. Using Eq. (13) and equation $\langle \chi_n | \hat{H} | \Psi \rangle = \langle \chi_n | E | \Psi \rangle$ we obtain

$$\sum_{j=0}^{M}(\mathcal{E}_j\delta_{nj} + V_{nj})c_j = Ec_n, \quad n = 0, 1, \ldots, M, \tag{14}$$

where $M \to \infty$ and $V_{nj} = \frac{1}{2}\langle \chi_n | \sum_{\substack{k,l=1 \\ k\neq l}}^{N} V(x_k - x_l) | \chi_j \rangle$. In practice $M+1 = \binom{N_{\max}}{N}$, where $N_{\max}$ is the number of the considered single-electron levels ε_{n_i}. System (14) determines the eigenvalues E_l and eigenvectors $(c_0^l, c_1^l, \ldots, c_M^l)$ for $l = 0, 1, \ldots, M$. We obtain the ground-state energy $E_{l=0}$ and ground-state wave function $\Psi_{l=0}$ by solving the system numerically.

TABLE I. The parameters V_0 and d used in the calculations of Fig. 1 and the values of α_{RG} and α resulting from formulas (15) and (5). Note that here $d \lesssim 1/2k_F \simeq 3$ nm. The last column ascribes a symbol to each set (V_0, d, α_{RG}).

V_0 (meV)	d (nm)	α_{RG}	α	Symbol in Fig. 1
11	3	0.0277	0.0273	○
34	3	0.0855	0.0821	○
68	3	0.171	0.158	○
1068	1	0.171	0.158	□
102	3	0.2565	0.230	○
1602	1	0.2565	0.230	□
11957	0.5	0.2565	0.230	△
2137	1	0.342	0.298	□
15942	0.5	0.342	0.298	△
3142	1	0.5	0.414	□
23445	0.5	0.5	0.414	△

If we use this full CI method (FCI) for a reasonable $N_{\max}$, a numerical solution of Eq. (14) is feasible for $N \lesssim 8$. Fortunately, expansion (13) still contains the terms which can be neglected. Our first approach, referred to as FCI, approximates the full CI as follows. We choose $N_{\max}$ and construct expansion (13) by adding first the Slater determinant of the ground state, then all determinants with a single excited electron, all determinants with two excited electrons, all determinants with three excited electrons, etc. If the resulting current [Eq. (10)] does not change, we cut the expansion by stopping to excite the electrons. Our second approach, introduced by two of us,[15] is the bucket-brigade CI method (BBCI). After choosing $N_{\max}$ one has to assess the importance of the $M+1$ determinants in expansion (13). Within the BBCI, the energy $\langle \chi_n | \hat{H} | \chi_n \rangle$ is chosen to define a measure of importance for each χ_n, enabling us to construct recursively a set of relevant determinants. (Increasing values of $\langle \chi_n | \hat{H} | \chi_n \rangle$ are assumed to correspond to decreasing importance.) As a result, expansion (13) is properly reordered and truncated. We increase the cutoff until the current saturates at a stable value.[12]

We use parameters typical for a GaAs ring, the electron effective mass $m = 0.067m_0$ and the density $N/L = 5 \times 10^7$ m^{-1}. The Fourier transform of Eq. (8) is $V(q) = 2V_0d/(1+q^2d^2)$. If this formula is used in Eq. (4), we obtain

$$\alpha_{RG}(V_0, d) \equiv 4V_0mk_Fd^3/\pi\hbar^2(1+4k_F^2d^2). \tag{15}$$

Using various sets (V_0, d, α_{RG}) listed in Table I, in Fig. 1 the persistent current in the ring with a single weak link is calculated as a function of the ring size. The top panel shows the BBCI data. For any α_{RG}, the BBCI data approach at large L the linear slope (dashed lines); i.e., they show the power law $LI \propto L^{-\alpha}$ or equivalently $LI \propto N^{-\alpha}$. Note, however, that the BBCI data for a given value of α_{RG} do not depend on d. This means that they cannot be fitted by the d-dependent formula (6). So we propose the d-independent expression (11). The

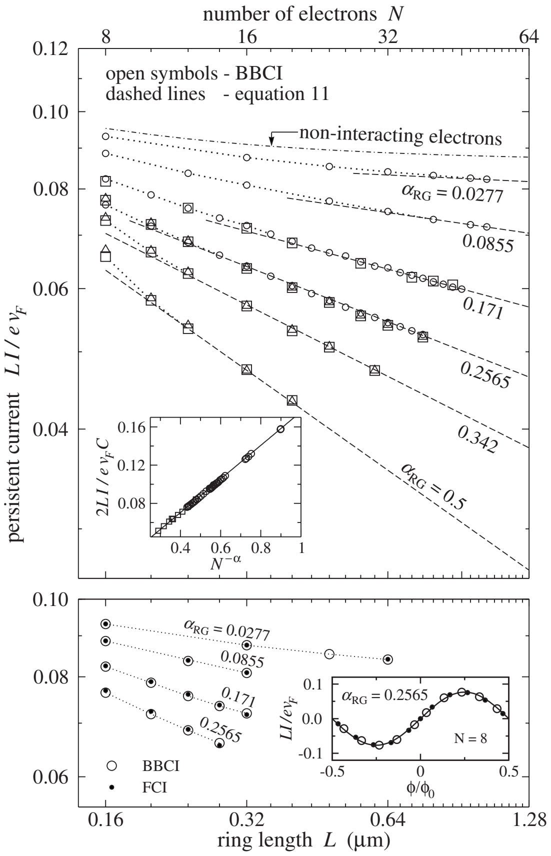

FIG. 1. Persistent current LI/ev_F versus L and N for $\phi=0.25\phi_0$. The transmission of the weak link is $|\tilde{t}_{k_F}|^2=0.03$. The top panel shows the BBCI results for various $(V_0,d,\alpha_{\mathrm{RG}})$ listed in Table I. The numerical result for noninteracting electrons (dotted-dashed line) approaches at large L the value $0.5|\tilde{t}_{k_F}|$, predicted for $\phi=0.25\phi_0$ by formula (1). The dashed lines show dependence (11), where $\alpha=(1+2\alpha_{\mathrm{RG}})^{1/2}-1$, α_{RG} is given by formula (15), and $C=1+1.66\alpha$. The BBCI data reach this asymptotic dependence at large N. Inset in the top panel shows the asymptotic BBCI data plotted as $2LI/ev_FC$ versus $x\equiv N^{-\alpha}$. The full line in inset is the function $f(x)=x|\tilde{t}_{k_F}|/|\tilde{r}_{k_F}|$. In the bottom panel we compare the selected BBCI data from the top panel with the FCI data. Inset in the bottom panel shows that the data follow the dependence $\propto\sin(2\pi\phi/\phi_0)$, drawn in the full line. The dotted lines are a guide for the eyes.

dashed lines show formula (11) for α calculated (Table I) from Eqs. (5) and (15). It is easy to see that the proportionality constant C has to be the same for various d at the same value of $\alpha_{\mathrm{RG}}(V_0,d)$. This means that C can depend only on α_{RG} (or on α), not on d. The simplest guess is $C=1+A\alpha$. If we choose $C=1+1.66\alpha$, formula (11) fits the CI data at large N for all considered $(V_0,d,\alpha_{\mathrm{RG}})$. The number $A=1.66$ is thus universal.

The inset in the top panel shows the asymptotic BBCI data normalized as $2LI/ev_F(1+1.66\alpha)$ and plotted in dependence on $x\equiv N^{-\alpha}$. For all considered $(N,V_0,d,\alpha_{\mathrm{RG}})$, the data collapse to a single curve $f(x)=x|\tilde{t}_{k_F}|/|\tilde{r}_{k_F}|$, representing Eq. (11). This is a sign of the power law $N^{-\alpha}$ with the numerical value of α being constant for all (V_0,d) obeying the equation $\alpha_{\mathrm{RG}}(V_0,d)=\mathrm{const}$.

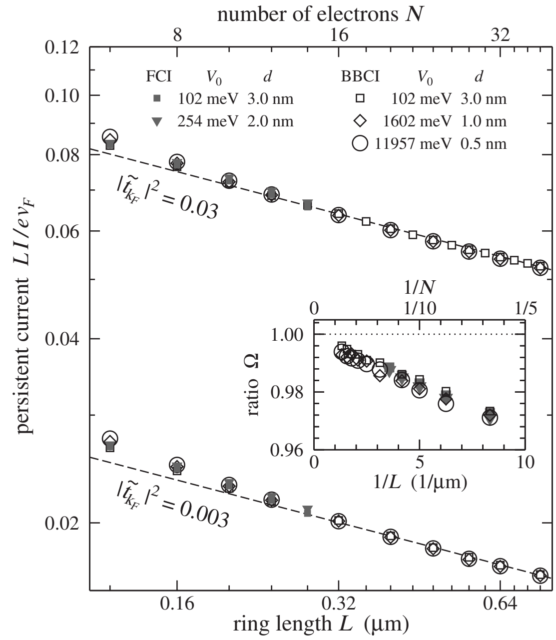

FIG. 2. Persistent current LI/ev_F versus L and N for $\phi=0.25\phi_0$. We compare the CI results for two different transmissions $|\tilde{t}_{k_F}|^2$ and for various interactions with (V_0,d) obeying the equation $\alpha_{\mathrm{RG}}(V_0,d)=0.2565$. The dashed lines show formula (11). Inset shows the CI data plotted as the ratio Ω (see the text), where $I(\tilde{t}_{k_F,1})$ and $I(\tilde{t}_{k_F,2})$ are the persistent currents for $|\tilde{t}_{k_F,1}|^2=0.03$ and $|\tilde{t}_{k_F,2}|^2=0.003$.

In the bottom panel we compare the selected BBCI data and FCI data. The inset in the bottom panel documents that the CI data oscillate as $\sin(2\pi\phi/\phi_0)$. The FCI provides independent verification of the BBCI but it cannot treat so large rings and so strong interactions.

Figure 2 compares the currents for two different $|\tilde{t}_{k_F}|^2$. Again, the CI data at large N follow the dependence [Eq. (11)] shown in a dashed line. The data exhibit the same slope for both transmissions, which means that α is independent of $\tilde{t}_{k_F}$. As before, the numerical value of α is the same for any (V_0,d) obeying the equation $\alpha_{\mathrm{RG}}(V_0,d)=\mathrm{const}$. To show that also the factor C in Eq. (11) is independent of $\tilde{t}_{k_F}$, in the inset we plot the CI data as the ratio $\Omega\equiv\frac{|\tilde{t}_{k_F,2}|/|\tilde{r}_{k_F,2}|}{|\tilde{t}_{k_F,1}|/|\tilde{r}_{k_F,1}|}\frac{I(\tilde{t}_{k_F,1})}{I(\tilde{t}_{k_F,2})}$. Using formula (11) we find $\Omega=1$; the CI data give $\Omega\to1$ for $N\to\infty$.

Figure 3 shows the CI data for various (V_0,d) including $d=12$ and 24 nm, i.e., $d>1/2k_F\simeq3$ nm. For all (V_0,d) we have $\alpha_{\mathrm{RG}}(V_0,d)=0.2565$. The CI data are compared with Eqs. (6) and (11). As before, Eq. (11) fits the CI data for $d\leq3$ nm$\simeq1/2k_F$. However, it fails to fit the CI data for $d>1/2k_F$ as it depends only on α_{RG} while the CI data for $d>1/2k_F$ depend also on d.

Further, Fig. 3 shows that Eq. (6) fails to fit the CI data for $d\lesssim1/2k_F$. Clearly, for a fixed L the persistent current (6) becomes zero in the limit $d\to0$, whereas the CI data for $d\lesssim1/2k_F$ show a d-independent nonzero current. The inset of Fig. 3 shows how the dependence on d disappears for $d\lesssim1/2k_F$.

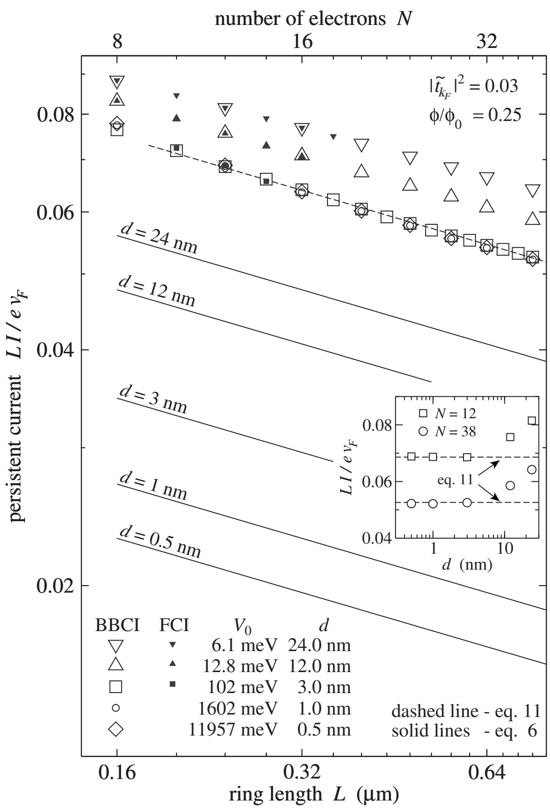

FIG. 3. Persistent current LI/ev_F versus L and N for various (V_0,d) chosen so that $\alpha_{RG}(V_0,d)=0.2565$ and $\alpha=(1+2\alpha_{RG})^{1/2}-1=0.23$. The CI data are compared with Eqs. (11) and (6). Equation (11) agrees with the CI data for $d\leq 3$ nm$\simeq 1/2k_F$ but fails to fit the CI data for $d>1/2k_F$ ($d=12$ and 24 nm) as they depend on d. To illustrate clearly how the dependence on d disappears for small d, the inset shows again the BBCI data for $N=12$ and $N=38$ but in dependence on d. Equation (6) does not fit the CI data (see the text for details).

Finally, Fig. 3 shows that formula (6) fails to fit the CI data for $d>1/2k_F$ (for $d=12$ and 24 nm). Of course, to fit the CI data for a given d, one might multiply the right-hand side of Eq. (6) by a proper numerical factor. It is however obvious that a different multiplication factor is needed for different d. Formula (6) multiplied by a single d-independent factor is expected (see below) to fit the CI data in the limit $L\gg d\gg 1/2k_F$, which is not feasible by our present CI methods.

To explain why our CI data for $d\lesssim 1/2k_F$ depend only on α_{RG} (not on d), we examine the matrix elements V_{ij}. Expressing V_{ij} by means of Eqs. (8) and (12) we obtain

$$V_{ij} = \frac{V_0}{2}\sum_{\alpha,\beta,\gamma,\delta} a_{ij}^{\alpha\beta\gamma\delta}\int_{-L/2}^{L/2} dx\,\psi_\alpha^*(x)\psi_\gamma(x) \times\int_{-L/2}^{L/2} dy\,e^{-|y|/d}\psi_\beta^*(x+y)\psi_\delta(x+y), \tag{16}$$

where $a_{ij}^{\alpha\beta\gamma\delta}$ is one of the values $\{-1,0,1\}$. We make use of the Taylor expansion

$$\int_{-L/2}^{L/2} dy\,e^{-|y|/d}f(x+y) = \sum_{n=0}^{\infty} v_n f^{(n)}(x), \tag{17}$$

where $v_n=\frac{1}{n!}\int_{-L/2}^{L/2}dy\,e^{-|y|/d}y^n$ and $f^{(n)}(x)=\frac{\partial^n}{\partial x^n}f(x)$. By means of simple algebra we express v_n as

$$v_n = \frac{1}{n!}[1+(-1)^n]\int_0^{L/2} dy\,e^{-|y|/d}y^n = d[1+(-1)^n]\left[d^n - e^{-L/2d}\sum_{m=0}^{n}\frac{d^m(L/2)^{n-m}}{(n-m)!}\right] \tag{18}$$

and we set it back into Eq. (17). Reordering the summations over m and n, identifying the particular Taylor series of $f^{(n)}(x\pm L/2)$, and applying the periodic condition $f^{(n)}(x\pm L)=f^{(n)}(x)$, we obtain from Eq. (17) the equation

$$\int_{-L/2}^{L/2} dy\,e^{-|y|/d}f(x+y) = 2d\sum_{n=0}^{\infty} d^{2n}[f^{(2n)}(x) - e^{-L/2d}f^{(2n)} \times(x-L/2)]. \tag{19}$$

Finally, for $L\gg d$ Eq. (19) simplifies to

$$\int_{-L/2}^{L/2} dy\,e^{-|y|/d}f(x+y) \approx 2d\sum_{n=0}^{\infty} d^{2n}f^{(2n)}(x). \tag{20}$$

Expressing the second integral in Eq. (16) by means of Eq. (20), we obtain the matrix element in the form[16]

$$V_{ij} \approx V_0 d\frac{L}{2\pi}\sum_{n=0}^{\infty}\left(\frac{2\pi d}{L}\right)^{2n}\sum_{\alpha,\beta,\gamma,\delta} a_{ij}^{\alpha\beta\gamma\delta} \times\int_{-\pi}^{\pi} dz\,\psi_\alpha^*(z)\psi_\gamma(z)\frac{\partial^{2n}}{\partial z^{2n}}[\psi_\beta^*(z)\psi_\delta(z)], \tag{21}$$

where $z=2\pi x/L$. The term with $n=0$ corresponds to the δ-function-like e-e interaction. Due to the Pauli principle, this term does not contribute to the energy and current. The next term is proportional to d^3. We use Eq. (15) to express V_0 via the parameters α_{RG} and d. We see that the matrix elements V_{ij} exhibit two special limits. In the limit $4k_F^2d^2\ll 1$, where $V_0\sim\alpha_{RG}/d^3$, the leading term in the summation over n is a d-independent constant. This explains why our CI data for $d\lesssim 1/2k_F$ show for fixed α_{RG} the d-independent current. In the limit $4k_F^2d^2\gg 1$, where $V_0\sim\alpha_{RG}/d$, the summation involves the terms $\propto d^2$, $\propto d^4$, etc., which means that the matrix element is a complicated function of d. Indeed, as d exceeds $1/2k_F$, our CI data show for fixed α_{RG} the current dependent on d.

We summarize the results of our continuous model. If $d\lesssim 1/2k_F$, the persistent current through the weak link with transmission $\tilde{t}_{k_F}$ is described by Eq. (11), where the power α agrees with the results of the Luttinger-liquid and RG models [formulas (5) and (4)]. Equation (11) implies the power law $LI/ev_F\simeq|\tilde{t}_{k_F}|N^{-\alpha}$, i.e., the interaction modifies $\tilde{t}_{k_F}$ as $t_{k_F}\simeq\tilde{t}_{k_F}N^{-\alpha}$.

Unlike these power laws, the Luttinger-liguid and RG models[3,5,6] predict the power laws $t_{k_F}\simeq\tilde{t}_{k_F}(L/d)^{-\alpha}$ and

$LI/ev_F \simeq |\tilde{t}_{k_F}|(L/d)^{-\alpha}$ [Eq. (6)], both depending on two interaction parameters, α and d. To explain why the power laws $t_{k_F} \simeq \tilde{t}_{k_F} N^{-\alpha}$ and $LI/ev_F \simeq |\tilde{t}_{k_F}| N^{-\alpha}$ do not depend on d, we have shown that the interaction-matrix elements V_{ij} depend in the limit $4k_F^2 d^2 \ll 1$ only on the interaction parameter α_{RG}.

We stress that our analysis of V_{ij} is not restricted to the continuous model. Indeed, the single-particle states ψ_n in Eq. (21) could in principle be the solutions of the lattice model or the eigenstates of the Hamiltonian with linear energy spectrum like the Luttinger-liquid model.[16] The power laws $t_{k_F} \simeq \tilde{t}_{k_F} N^{-\alpha}$ and $LI/ev_F \simeq |\tilde{t}_{k_F}| N^{-\alpha}$ should therefore arise also in the Luttinger-liquid and RG models but in the limit $4k_F^2 d^2 \ll 1$ $(d \lesssim 1/2k_F)$. Most likely, the power laws $t_{k_F} \simeq \tilde{t}_{k_F}(L/d)^{-\alpha}$ and $LI/ev_F \simeq |\tilde{t}_{k_F}|(L/d)^{-\alpha}$ are valid in the opposite limit, $d \gg 1/k_F$, and we expect them to appear for large enough d also in our continuous model.

More precisely, we expect that the two-parametric formula (6) (with the right-hand side multiplied by a proper d-independent constant of the order of unity) would agree with the CI results obtained in the limit $d \gg 1/k_F$. Indeed, as d exceeds $1/2k_F$, our CI results (Fig. 3) start to depend on both d and α. Unfortunately, to verify the two-parametric dependence $LI/ev_F \simeq |\tilde{t}_{k_F}|(L/d)^{-\alpha}$, we actually need to reach the limit $L \gg d \gg 1/2k_f$. Our present CI methods do not allow to reach that limit numerically due to computational reasons.

Concerning result (5), it was derived[7] from the Luttinger-liquid model[1] in order to generalize the weak-interaction RG result [Eq. (4)]. We have verified both results in the continuous model for various $d \lesssim 1/2k_F$. This suggests that both results are model independent, no matter whether the dispersion is linear or parabolic.

Finally, an interesting result in all our figures is that the $N^{-\alpha}$ limit is reachable for $N \sim 10$. This means that already ten electrons can behave as a Luttinger liquid. The effect is due to the very weak link combined with a proper interaction ($\alpha_{\mathrm{RG}} \gtrsim 0.25, d \lesssim 1/2k_F$) and might be observable in the GaAs 1D systems, where a realistic calculation of screened interaction[12] confirms quite well the exponential screening with $d \simeq 1/2k_F$. Of course, it might be interesting to extend our CI calculations to the short-ranged interactions with a shape differing from the exponential one.

The IEE group was supported by the Grant Agency APVV (Grants No. APVV-51-003505, No. VVCE-0058-07) and Grant Agency VEGA (Grant No. VEGA-2/6101/27).

[1] J. Voit, Rep. Prog. Phys. **58**, 977 (1995).
[2] Y. Imry, *Introduction to Mesoscopic Physics* (Oxford University Press, Oxford, UK, 2002).
[3] C. L. Kane and M. P. A. Fisher, Phys. Rev. Lett. **68**, 1220 (1992).
[4] Z. Yao, H. W. Ch. Postma, L. Balents, and C. Dekker, Nature (London) **402**, 273 (1999).
[5] A. O. Gogolin and N. V. Prokof'ev, Phys. Rev. B **50**, 4921 (1994).
[6] K. A. Matveev, D. Yue, and L. I. Glazman, Phys. Rev. Lett. **71**, 3351 (1993); D. Yue, L. I. Glazman, and K. A. Matveev, Phys. Rev. B **49**, 1966 (1994).
[7] D. G. Polyakov and I. V. Gornyi, Phys. Rev. B **68**, 035421 (2003).
[8] V. Meden and U. Schollwöck, Phys. Rev. B **67**, 035106 (2003).
[9] T. Enss, V. Meden, S. Andergassen, X. Barnabé-Thériault, W. Metzner, and K. Schönhammer, Phys. Rev. B **71**, 155401 (2005).
[10] V. Meden, T. Enss, S. Andergassen, W. Metzner, and K. Schonhammer, Phys. Rev. B **71**, 041302(R) (2005).
[11] S. Andergassen, T. Enss, V. Meden, W. Metzner, U. Schollwöck, and K. Schönhammer, Phys. Rev. B **73**, 045125 (2006).
[12] R. Németh, M. Moško, R. Krčmár, A. Gendiar, K. M. Indlekofer, and L. Mitas, arXiv:0902.2225 (unpublished).
[13] A. Szabo and N. S. Ostlund, *Modern Quantum Chemistry: Introduction to Advanced Electronic Structure Theory* (Dover Publications, Mineola, NY, 1996).
[14] J. C. Greer, J. Comput. Phys. **146**, 181 (1998).
[15] K. M. Indlekofer, R. Németh, and J. Knoch, Phys. Rev. B **77**, 125436 (2008).
[16] Expression (21) holds for any single-particle wave function ψ as long as the derivative $\frac{\partial^{2n}}{\partial z^{2n}}[\psi_\beta^*(z)\psi_\delta(z)]$ exists for $n=1,2,\ldots$.